Available online at www.sciencedirect.com

SCIENCE DIRECT®

Thin Solid Films 494 (2006) 173 – 178

thin solid films

www.elsevier.com/locate/tsf

Effect of heat treatment on mechanical properties and microstructure of CrN/AlN multilayer coatings

Shih-Kang Tien, Jenq-Gong Duh *

Department of Materials Science and Engineering, National Tsing Hua University, Hsinchu, Taiwan

Available online 9 September 2005

Abstract

Polycrystalline CrN/AlN multilayer coatings were deposited by RF magnetron sputtering on silicon (001) substrates. The bilayer periods of CrN/AlN were controlled from 4 nm to 20 nm by the use of shutters, which were adjusted by a programmable logic control (PLC). To evaluate the thermal stability, the films were annealed at 500 °C, 600 °C, 700 °C, 800 °C, and 850 °C, for 1 h in both vacuum and air environments. The phase transformation during thermal evolution was studied by X-ray diffraction (XRD). The microstructure of CrN/AlN multilayer coatings as-deposited and after annealing was observed by transmission electron microscopy (TEM). The hardness of as-deposited CrN/AlN coating with a period of 4 nm was 28.2 GPa, which was 60% higher than that predicted by the rule of mixtures. The hardness of CrN/AlN multilayer coatings annealed at 850 °C in vacuum remained similar to the as-deposited state, and the nano-layered structure still persisted. The thermal stability of CrN/AlN coatings was better than that of CrN coating. The hardness degradation ratio of CrN/AlN coating with modulation period of 4 nm was only 8.1% at 700 °C, which was superior to that of a simple CrN coating.

Keywords: CrN; AlN; Multilayer coating; Thermal stability; Hard coating

1. Introduction

Multilayer coatings composed of two kinds of transition nitride films have been investigated in recent years, and these have been found to exhibit superior mechanical and chemical properties, such as hardness, adhesion, and wear resistance, when compared to single layer nitride coatings [1–7]. Although multilayer coatings can possess high hardness at an ambient temperature, heat treatment at elevated temperatures in vacuum has been reported to degrade the strength of multilayer coatings leading to failure. This is a critical issue which is caused by the disappearance of the nano-layered structure due to the inter-diffusion of atoms [8–12]. It was also found that when annealed in air, the hardness of the multilayer coatings was reduced even below the hardness of the rule of mixtures because of significant oxidation on the top of films [13–15]. As a result, thermal stability plays an important role in the performance of coated tools operated at elevated temperature in either vacuum or air. CrN films, which have been studied for many years, demonstrate good mechanical performance, thermal properties and anti-oxidation behavior [16,17]. Also, AlN may also be of interest, since Al_2O_3 may form to protect the coating at elevated temperatures. It has been suggested that CrN/AlN multilayer coatings could have enhanced hardness, as compared with CrN [18]. This study was mainly focused on the thermal stability of CrN and CrN/AlN coatings with modulation periods of 4 nm and 20 nm in both vacuum and air environments. Comparison between coatings at vacuum and air will be discussed. The microstructure of CrN and CrN/AlN coatings were analyzed by X-ray diffraction, SEM and TEM. Nanoindentation tests were used to investigate the hardness of the films deposited under various conditions.

2. Experimental

CrN and multilayered CrN/AlN coatings with different modulation periods were deposited on silicon substrates by RF magnetron sputtering. The chromium and aluminum sputtering targets were 50.8 mm in diameter and 99.95 wt.% in purity. The working distance for both sputtering guns was 60.0 mm. After loading substrates and targets, the

* Corresponding author. Fax: +886 3 5712686.
E-mail address: jgd@mx.nthu.edu.tw (J.-G. Duh).

0040-6090/$ - see front matter © 2005 Elsevier B.V. All rights reserved.
doi:10.1016/j.tsf.2005.08.198

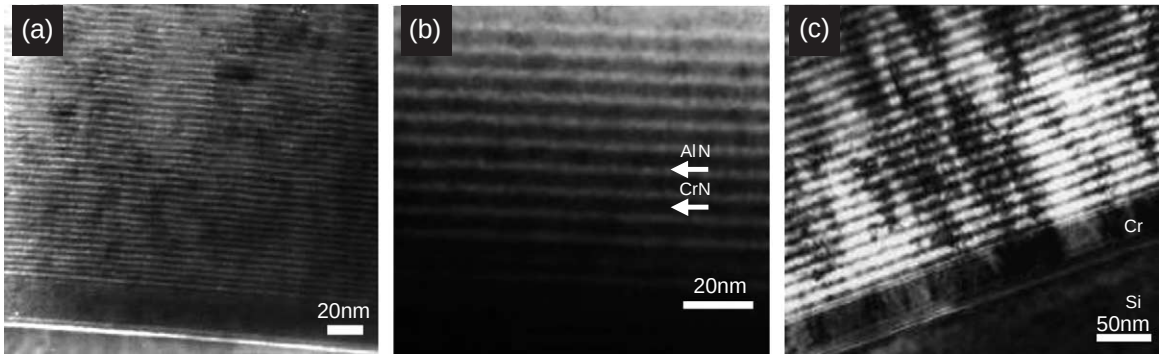

Fig. 1. Bright field image of CrN/AlN coatings with modulation period of (a) 4 nm, (b) 6.7 nm and (c) 10 nm.

deposition chamber was pumped down to 8.0×10^{-4} Pa. The substrate temperature was 300 °C and rotation speed was 20 rpm during deposition. The target power was 150 W for Cr and 100 W for Al. A 40 nm layer of Cr was coated on the Si substrate to enhance the adhesion strength between substrate and nitride coatings. Argon was utilized at 2.0×10^{-1} Pa. Nitrogen gas was also used for reactive sputtering at a working pressure of 2.0×10^{-1} Pa. Multilayer CrN/AlN coatings were prepared with different bilayer periods ranging from 4 nm to 20 nm. The thickness of each layer was decided by the switch time of alternate shutters, which were controlled by a programmable logic control (PLC). The thickness ratio

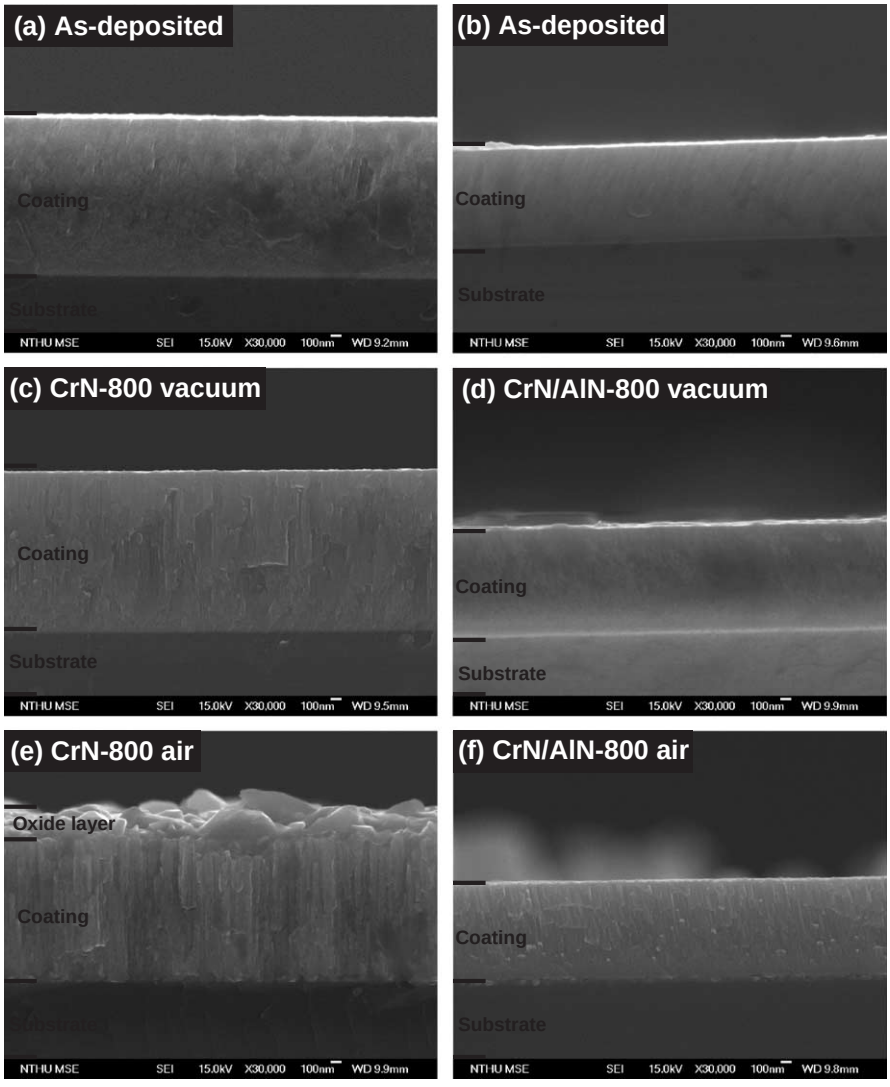

Fig. 2. SEI micrographs of various coatings (a) CrN, as-deposited; (b) CrN/AlN, as-deposited; (c) CrN, 800 °C in vacuum; (d) CrN/AlN, 800 °C in vacuum; (e) CrN, 800 °C in air; (f) CrN/AlN, 800 °C in air.

of CrN to AlN was fixed at 1.0. After deposition, the CrN and CrN/AlN multilayer coatings were annealed in vacuum and air at temperatures from 500 °C, 600 °C, 700 °C, 800 °C and 850 °C, for 1 h. The heating rate of the furnace was controlled at 10 °C/min.

The microstructure and modulation period of the multilayer CrN/AlN coatings were observed by transmission electron microscopy (JSM-2010, JEOL, Japan). For the TEM analysis, the film was first ground, and then transferred onto a Cu grid. A Gatan dual ion mill with incident angle of 3–8° and 4.5 keV was utilized to create samples thin enough for electron transparency. An X-ray diffractometer (Shimadzu, XRD6000, Japan) with continuous $\theta-2\theta$ scan was used to identify phase transformations in the coating after heat treatment. Cu K_α radiation with a wavelength of 0.15418 nm was generated from a Cu target operated at 40 kV and 30 mA. The high angle 2θ scan ranged from 30° to 60° with a step width of 0.02° at 3°/min. The multilayer structure was also detected by low angle X-ray diffraction from 2° to 9° [19–22]. The cross-sectional microstructure and the thickness of coatings were evaluated by FESEM (JSM-6500, JEOL, Japan). The hardness of films was analyzed by nanoindentation (Triboscope, Hysitron, Minneapolis, MN) technique. The load was fixed at 5 mN and the indentation depth was below 1/10 of the coating thickness.

3. Results and discussion

3.1. Microstructure and phase identification

Fig. 1 shows TEM micrographs of the CrN/AlN multilayer coatings with different modulation periods. The bright and dark layers represent alternate AlN and CrN coatings, respectively, the thickness ratio of CrN to AlN measured from bright field image was fixed at 1.0 for CrN/AlN multilayer coatings with different modulation periods. The interface between CrN and AlN was flat and evident. A native oxide layer around 4 nm was also found on the Si substrate.

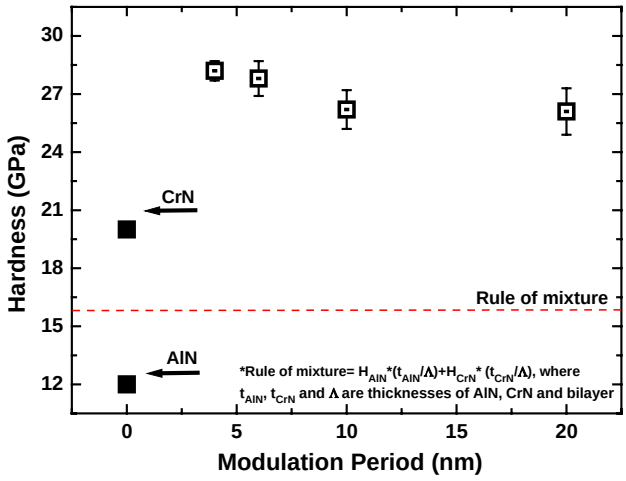

Fig. 4. Hardness of CrN/AlN coatings as a function of modulation period.

The cross-sectional view of CrN and CrN/AlN coatings are shown in Fig. 2. The thickness of CrN and CrN/AlN coatings estimated from the SEM image were 1.3 and 0.9 μm, respectively. The microstructure of the as-deposited CrN coating exhibited a fine-grained dense morphology. Conversely, the CrN/AlN multilayer coatings showed a dense columnar structure. After heat treatment at 800 °C in vacuum for 1 h, the cross-sectional microstructure of the CrN coating transformed from a fine-grained morphology to a dense columnar structure. The multilayer coatings still maintained a dense columnar structure after 800 °C in vacuum for 1 h. On the other hand, the cross-section view of a CrN coating exhibited not only loose but also rough morphology after 800 °C in air with the same time as that in vacuum. In fact, the interface between CrN and oxide layer could not be distinguished. A similar phenomenon was observed by

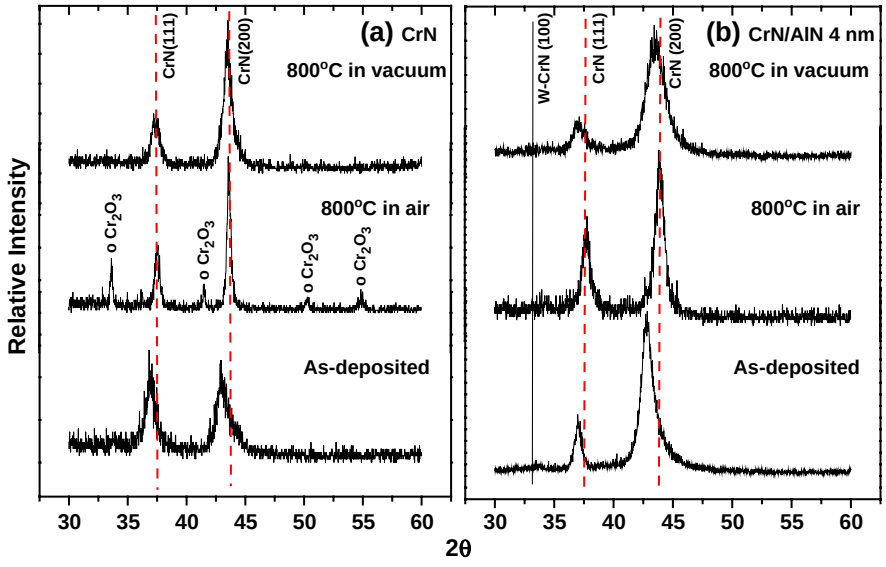

Fig. 3. X-ray diffraction patterns of (a) CrN, (b) CrN/AlN with 4 nm period at as-deposited state, 800 °C in air and 800 °C in vacuum.

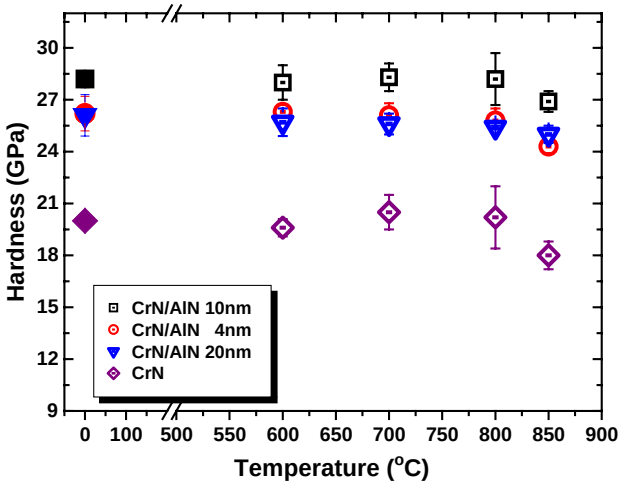

Fig. 5. Hardness of CrN and CrN/AlN coatings as a function of annealing temperatures in vacuum for 1 h.

Ichimura [17]. Nevertheless, the SEM micrograph of multilayer CrN/AlN coatings in Fig. 2(f) still possessed a dense columnar structure equivalent to that after heat treatment in air at 800 °C for 1 h.

The X-ray diffraction patterns of CrN and CrN/AlN with 4 nm coatings at as-deposited and heat treatment states are shown in Fig. 3. The diffraction peaks of the as-deposited CrN coating located at 36.98° and 42.96° are CrN (111) and CrN (200), respectively, which were shifted toward lower angles. The reason for the peak shift was a compressive stress in the CrN coating. The diffraction patterns of as-deposited CrN/AlN coatings with 4 nm showed f.c.c. CrN/AlN structure, and no wurtzite AlN structure was observed. This indicated that the hexagonal structure of AlN was transformed into the metastable cubic structure as the modulation period of multilayer CrN/AlN was 4 nm [4,10,18]. As shown in Fig. 3(a), the diffraction pattern of CrN coating at 800 °C in vacuum became sharper as compared with the as-deposited coating. The CrN/AlN coatings still exhibited broad peaks, implying that the grain size of film did not grow. In fact, the major CrN (111) and CrN (200) for CrN and CrN/AlN coatings all move toward higher angle, indicating stress relaxation after heat treatment. The CrN coating was oxidized and Cr_2O_3 was formed during annealing at 800 °C in air for 1 h, while no Cr_2O_3 peak in the CrN/AlN coatings could be found. Therefore, the CrN/AlN coating possessed better thermal stability than CrN coating if oxidation is a concern.

3.2. Mechanical properties and thermal stability

The hardness of nitride coatings are exhibited in Fig. 4. The hardness of CrN and AlN coatings was 20.0 GPa and 12.0 GPa, respectively. However, the hardness of CrN/AlN multilayer coatings fabricated by the sequential deposition of CrN and AlN layers increased up to 30 GPa, which was much larger than that predicted by the rule of mixture. It is argued that there seems to be some correlations between the hardness of multilayer coating and the modulation period [13]. In this study also the hardness increased with reducing the modulation period. The hardness enhancement of CrN/AlN coatings with modulation period of 4 nm and 20 nm was 76.3% and 63.1%, respectively. The significant enhancement in hardness of the CrN/AlN stack was attributed to many interfaces that blocked the dislocation movement [23].

Fig. 5 presents the hardness of CrN and CrN/AlN multilayer coatings as a function of annealing temperature from 600 °C to 850 °C for 1 h in vacuum. The chamber was evacuated down to 2×10^{-6} Torr to prevent oxidation of the films. The heating rate was fixed at 10 °C/min, which was the same as the heat treatment in air. The hardness of CrN and CrN/AlN coatings after heat treatment in the range between 600 °C and 800 °C for

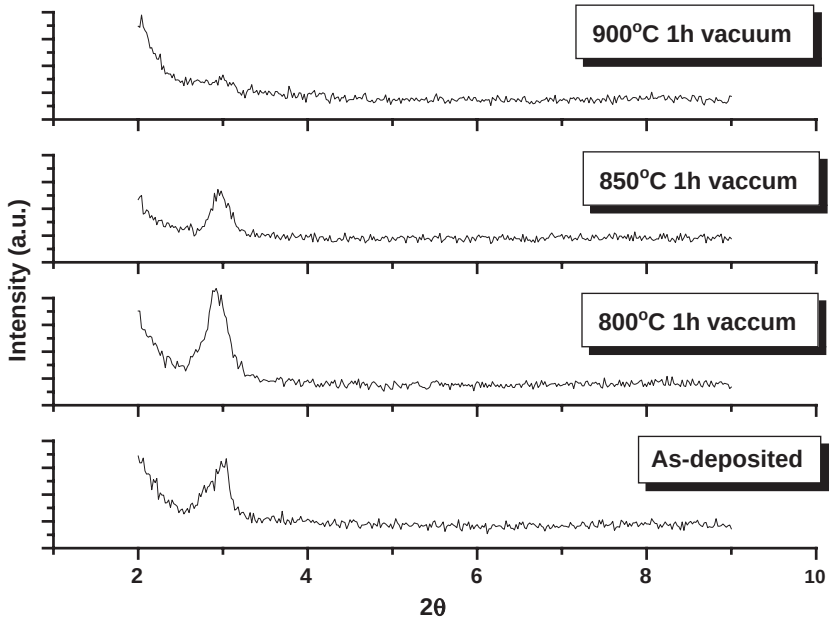

Fig. 6. Hardness of CrN and CrN/AlN coatings as a function of annealing temperatures in air for 1 h.

1 h in vacuum retained a high strength and no degradation was detected.

The CrN/AlN multilayer coating, with a modulation period of 4 nm in the as-deposited and heat treated states, was investigated by the low angle X-ray diffraction patterns, as illustrated in Fig. 6. The sharp diffraction peak of the as-deposited CrN/AlN coating located near 3° indicated the existence of multilayer structure, which was consistent with the result of TEM. During heat treatment, the low angle X-ray diffraction pattern still existed at 850 °C for 1 h, implying that the bilayer structure of multilayer coating did not vanish. Moreover, the intensity of the low angle diffraction peak remained unchanged below 800 °C. Nevertheless, the peak intensity gradually decreased above 800 °C at annealing temperature. It was suggested that the vanishing of the multilayer coating was due to the inter-diffusion of each layer [10]. When heated up to 900 °C for 1 h, the low angle X-ray diffraction pattern disappeared, which resulted from a tensile crack in the film due to the difference in thermal expansion coefficient between Si and CrN/AlN coatings.

Fig. 7 plots the relationship between the hardness of a single layer CrN coating and multilayered CrN/AlN coatings with different modulation periods. The hardness of both CrN/AlN coatings was unchanged up to 500 °C for 1 h in air environment. However, the hardness of the CrN coating decreased rapidly to 9.9 GPa as the annealing temperature reached 700 °C. Relatively speaking, the decrease in hardness for the multilayer CrN/AlN coating was much slighter than that of CrN coating. The degradation ratios at 700 °C for CrN and CrNN/AlN with 4 nm were 50.5% and 8.1%, respectively. For annealing up to 800 °C, the hardness of the CrN coating could not be measured because of rougher surface morphology caused by severe oxidation. This could be seen from the X-ray diffraction analysis, and films were actually detached from the substrate.

The hardness of the multilayer coatings with 4 nm and 20 nm periods, after heat treatment at 800 °C, was maintained as high as 23.5±0.8 GPa and 20.2±0.2 GPa, respectively, which were only 16.7% and 22.6% lower than that of the as-deposited coatings. Harish reported that the hardness of TiAlN and TiN/AlN coatings exhibited hardness of 22 GPa and 28 GPa, which were 42.9% and 22.2% lower than that of as-deposited films after heating at 700 °C for 30 min in air [13]. Harish also presented that TiAlN/CrN multilayer coating with modulation period of 5.6 nm still exhibited 26 GPa at 800 °C and degradation ratio was 33.3% [14]. As a result, the CrN/AlN coatings could maintain excellent strength even when annealed at an elevated temperature in air.

For CrN and CrN/AlN coatings annealed in vacuum, the hardness of both coatings at various temperatures remained nearly unchanged; hardness decreased after annealing at 500 °C in air. The difference in hardness at identical temperatures may be due to the oxidation layer grown on the top of the coatings. Indentation testing with a load of 5 mN applied on the coating produced a maximum indentation depth for both coatings below 100 nm. As a result of the soft and loose oxide layer produced on the top of both coatings, the hardness of the coatings decreases significantly with annealing temperature. Thus, the ability to resist oxidation attack strongly affects the thermal stability of the coating at elevated temperatures in air.

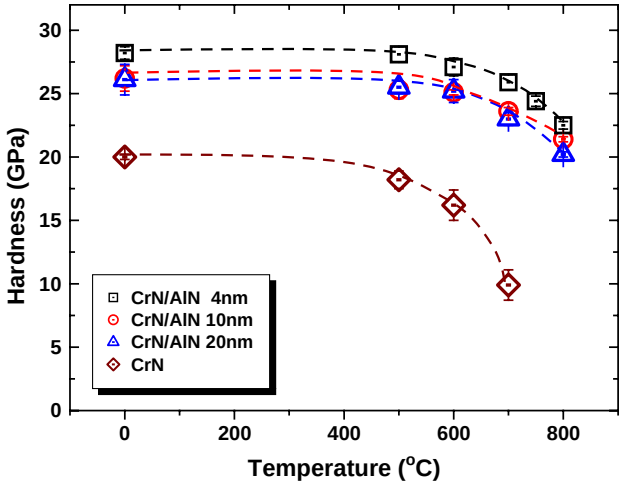

Fig. 7. Low angle X-ray diffraction patterns of CrN/AlN coating with modulation period of 4 nm before and after annealing at various temperatures in vacuum for 1 h.

4. Conclusions

CrN/AlN multilayer coatings with different modulation periods were fabricated by alternate depositions of CrN and AlN layers by RF magnetron sputtering. The enhancement in hardness was over 60% higher than that predicted by the rule of mixture. After 800 °C for 1 h in vacuum, the hardness of the CrN/AlN coating still remained unchanged and the microstructure retained a dense columnar structure and smooth top surface. The multilayer structure of CrN/AlN coating existed even after annealing at 850 °C for 1 h. In addition, the hardness of CrN/AlN coating with modulation period of 4 nm exhibited excellent thermal stability and formed a dense and smooth layer above the coating after treated at 800 °C for 1 h in air. The hardness of the single layer CrN coating decreased rapidly to 9.9 GPa after annealing in air at 600 °C, and the microstructure of CrN coating became rough and loose, due to severe oxidation. The hardness degradation ratios for CrN and CrN/AlN coatings with modulation period of 4 nm at 700 °C were 50.5% and 8.1%, respectively. As a result, the multilayer CrN/AlN coating possessed good mechanical strength and thermal stability at elevated temperatures in both vacuum and air environment.

Acknowledgment

Support for this work from the National Science Council, Taiwan, under Contract No. NSC 93-2216-E-007-013 is appreciated.

References

[1] U. Helmersson, S. Todorova, S.A. Barnett, J.E. Sundgren, L.C. Markert, J.E. Greene, J. Appl. Phys. 62 (1987) 481.
[2] X. Chu, S.A. Barnett, M.S. Wong, W.D. Sproul, Surf. Coat. Technol. 57 (1993) 13.

[3] H.Y. Lee, J.G. Han, S.H. Baeg, S.H. Yang, Thin Solid Films 420–421 (2002) 414.
[4] M. Setoyama, A. Nakayama, M. Tanaka, N. Kitagawa, T. Nomura, Surf. Coat. Technol. 86–87 (1996) 225.
[5] Y.Y. Wang, M.S. Wong, W.J. Chia, J. Rechner, W.D. Sproul, J. Vac. Sci. Technol., A 16 (1998) 3341.
[6] M.S. Wong, G.Y. Hsiao, S.Y. Yang, Surf. Coat. Technol. 133–134 (2000) 160.
[7] D.C. Cameron, R. Aimo, Z.H. Wang, K.A. Pischow, Surf. Coat. Technol. 142–144 (2001) 567.
[8] H.C. Barshilia, K.S. Rajam, Surf. Coat. Technol. 183 (2004) 174.
[9] Q. Yang, L.R. Zhao, J. Vac. Sci. Technol., A 21 (2003) 558.
[10] M. Setoyama, M. Irie, H. Ohara, Y. Takeda, T. Nomura, N. Kitagawa, Thin Solid Films 341 (1999) 126.
[11] D.G. Kim, T.Y. Seong, Y.J. Baik, Surf. Coat. Technol. 153 (2002) 79.
[12] L. Hultman, Vacuum 57 (2000) 1.
[13] H.C. Barshilia, A. Jain, K.S. Rajam, Vacuum 74 (2004) 241.
[14] H.C. Barshilia, M.S. Prakash, A. Jain, K.S. Rajam, Vacuum 77 (2005) 169.
[15] X.T. Zeng, S. Zhang, C.Q. Sun, Y.C. Liu, Thin Solid Films 424 (2003) 99.
[16] J.N. Tu, J.G. Duh, S.Y. Tsai, Surf. Coat. Technol. 133–134 (2000) 181.
[17] H. Ichimura, A. Kawana, J. Mater. Res. 9 (1994) 151.
[18] G.S. Kim, S.Y. Lee, J.H. Hahn, S.Y. Lee, Surf. Coat. Technol. 171 (2003) 91.
[19] L.A. Donohue, W.D. Munz, D.B. Lewis, J. Cawley, T. Hurkmans, T. Trinh, I. Petrov, J.E. Greene, Surf. Coat. Technol. 93 (1997) 69.
[20] C. Engstrom, J. Birch, L. Hultman, C. Lavoie, C. Cabral, J.L. Jordan-Sweet, J.R.A. Carlsson, J. Vac. Sci. Technol., A 17 (1999) 2920.
[21] A. Madan, I.W. Kim, S.C. Cheng, P. Yashar, V.P. Dravid, S.A. Barnett, Phys. Rev. Lett. 78 (1997) 1743.
[22] V. Pankov, M. Evstigneev, R.H. Prince, J. Vac. Sci. Technol., A 20 (2) (2002) 430.
[23] X. Chu, S.A. Barnett, J. Appl. Phys. 77 (1995) 4403.